Dielectric relaxation in sodium bis(2-ethylhexyl)sulfosuccinate–water–decane microemulsions near the percolation temperature threshold

Yuri Feldman, Nikolay Kozlovich, Ido Nir, and Nissim Garti
Casali Institute of Applied Chemistry, The Hebrew University of Jerusalem, 91904 Jerusalem, Israel
(Received 5 July 1994)

The results of an extensive study of percolation in order to verify some theoretical predictions about percolation critical indices for changes in static and dynamic dielectric properties of a microemulsion as a function of temperature and frequency are presented in this paper. The dynamic behavior of the microemulsions was also studied in order to reveal the mechanisms that are responsible for dielectric polarization of the system. The measurements were made by means of the time domain dielectric spectroscopy method in the frequency range 10^5–10^{10} Hz and at temperatures from 10 °C to 40 °C. It was shown in our study that critical indices for conductivity and dielectric permittivity have the values $s \approx 1.2$ below and $t \approx 1.9$ above the percolation threshold. The value for the critical index s is in agreement with a dynamic percolation picture. This confirms the idea that the mechanism responsible for the temperature dependence of conductivity and permittivity has the same origin. The numerical value of t indicates a percolation picture above the threshold; however, it does not provide information about the nature of percolation. The data treatment for the dynamic behavior of the microemulsions was carried out in the time domain in terms of dipole correlation functions. It was found that the correlation functions exhibit complex nonexponential relaxation behavior in the percolation region and must be deconvoluted into normal modes and represented as the sum of the simple exponential $\exp(-t/\tau)$ and nonexponential terms $\exp[-(t/\tau)^{\beta}]$. The frequency scaling parameters m, p, and u, as well as the stretched parameters in the time window β, provide information about the microstructure and dynamics of the system. The analysis of their temperature dependence shows the existence of spatial, temporal, and energetic disorder associated with anomalous diffusion of charge carriers in the percolation clusters. On the basis of a detailed analysis of the time relaxation data spectrum, the molecular dynamic mechanism of dielectric polarization in the percolation region was suggested.

PACS number(s): 82.70.−y, 77.22.Gm, 05.40.+j

I. INTRODUCTION

Microemulsions are systems that have been very widely studied during recent years because of their fundamental importance and their numerous practical applications. These systems are macroscopically single-phase, thermodynamically stable systems containing oil and water, stabilized by molecules of surfactant [1–3]. In the case of an oil-continuous (W-O) microemulsion, one possible structure is that of spherical water droplets surrounded by a monomolecular layer of surfactant molecules whose hydrophobic tails are oriented toward the continuous oil phase. There are also microemulsions in which the minor component forms disks, sheets, or rods, as well as mixtures that are bicontinuous [2–5]. When the molar ratio of water to surfactant $W = [\text{water}]/[\text{surfactant}]$ is kept constant, the water core has a permanent average radius [6,7] and the one-phase microemulsion shows a large variety of important physical phenomena when the temperature and volume fraction of the dispersed phase is varied.

If the surfactant is anionic, its molecules can dissociate into negatively charged head groups of hydrophilic nature and positive counterions. Under the influence of an electric field, these charges can accumulate on the inner surfaces of the micelles, giving rise to polarization processes and affecting the conductivity of the system.

A percolation phenomenon was found in a W-O microemulsion when the water fraction, the temperature, or the ratio of water to the surfactant was varied [8–25]. The occurrence of percolation reveals that droplet size, attractive interactions, and the rate of exchange of material between droplets through collisions increase. The percolation threshold corresponds to the formation of the first infinite cluster of droplets. The number of such clusters increases very rapidly above the percolation threshold, giving rise to the observed changes of the physical and chemical properties of the system.

Percolation can be manifested by a rapid increase in the dielectric constant and the conductivity of the microemulsion when the volume fraction ϕ of the dispersed phase (water plus surfactant) reaches a critical value ϕ_c at a constant temperature. A similar transition will occur when the temperature T reaches a value T_c at a constant ϕ or when the molar ratio of water to surfactant increases [9–15]. This rapid variation can be represented for conductivity by two separate asymptotic scaling power laws with exponents that are different above and below the percolation threshold [10–16].

From a theoretical point of view, two approaches have been proposed for the mechanism leading to percolation in microemulsions. The first approach, *the static percolation model,* attributes this phenomenon to the appearance of bicontinuous oil and water structures [5]. Based on

this model, the sharp increase of the electrical conductivity σ in such a microemulsion can be explained by a connected water path in the system. The second approach, *the dynamic percolation model,* considers the attractive interactions between water droplets as responsible for the formation of percolation clusters [9]. This model takes into account the effect of cluster rearrangements due to Brownian motion. In this dynamic picture, charge transport is ensured by the hopping or diffusing of charge carriers through clusters which rearrange with time.

It has been conjectured that below the percolation threshold, dynamic percolation takes place, which relates the observed effect to hopping of surfactant molecules (anions) or counterions (cations) within transient clusters formed by microemulsion droplets [9,10]. The electrical conductivity above the percolation threshold volume fraction or temperature has been attributed to two possibilities: the "hopping" of surfactant ions from droplet to droplet within droplet clusters or the transfer of counterions from one droplet to another through water channels formed in droplet clusters. These channels are formed when surfactant layers separating adjacent water cores open up during collisions or through the transient merging of droplets [26–29].

The interdroplet interaction accounts for the thermal phase separation in microemulsions. Xu and Stell [30] calculated the locus of the percolation threshold using a model hard-sphere system with an attractive Yukawa tail in the mean spherical approximation. They introduced a pair-correlation function that is proportional to the probability of finding two particles at a distance r apart in the same cluster. They constructed and solved in a mean spherical approximation the Ornstein-Zernike equation for this function. By solving this equation one can calculate the percolation threshold, the average cluster size, and the cluster size distribution. The percolation transition threshold is the state at which the average cluster size becomes divergent. The general study of correlated site-bond percolation in microemulsions on the microscopic lattice models was developed by Skaf and Stell [31,32]. The formalism presented in these papers is a microscopic one, which within a mean-field approximation enables one to study the effect of structure, composition, interparticle interaction, salinity, etc., on the clustering properties of microemulsions.

There are several physical methods that can provide precise information about the structure and dynamic processes that occur in complicated multiphase systems such as microemulsions. Among others, we can mention light, x-ray, and neutron scattering, NMR, electron spin resonance, calorimetric techniques, ultrasound, and dielectric spectroscopy [10–29, 33–37]. The latter is a direct tool for the investigation of different kinds of microstructures and depends on charged or polar interfaces. Both time domain dielectric spectroscopy (usually called TDDS) [37] as well as frequency domain methods [15] can be used to determine significant characteristics of such systems, microemulsions in particular, over a wide temperature and frequency range.

The times proved by the TDDS method (10^{-5}–10^{-10} s) are located between those of mechanical measurements (lower than 10^{-5} s) and those of Brillouin light, neutrons, and Raman scattering (10^{-9}–10^{-14} s). This time window covers a broad region, which includes some characteristic relaxation times representing the polarization of microdroplets and clusters, interdroplet exchange of matter, and aggregation processes in microemulsions.

The dynamic aspects of percolation are taken into account by introducing a time or frequency scale. It was suggested [10–15] that relaxation process connected with percolation might only be characterized using a complex spectrum of relaxation times. The frequency dependence of the dielectric constant is found to deviate from the Debye relaxation [8,10] and the time correlation function of the droplet density fluctuation deviates from an exponential decay. The density correlation function follows a stretched law of the Kohlrausch-Williams-Watts [33,34] type, which is related to the existence of a constrained diffusion of matter in the percolation cluster of the microemulsion.

The percolation clusters are self-similar [38] and they can be modeled by fractal structures. The theory of dynamics in fractal systems and on percolation clusters has been treated many times in literature [38–40], but only a few experimental studies have been undertaken to investigate the theoretical predictions concluded from those papers. The verification and check of the specific features of molecular dynamics and transport processes expected for self-similar structures such as microemulsions in the percolation region still remains to be done, as well as to obtain information about their polarization and dielectric relaxation properties.

It is the purpose of this paper to present a comprehensive study of the dielectric properties of sodium bis(2-ethylhexyl)sulfosuccinate (AOT)–water–decane microemulsions near the percolation temperature threshold by the time domain dielectric spectroscopy method. The presented experimental results, covering the broad time window (10^{-5}–10^{-10} s) and temperature range (10 °C–40 °C), allow us to gain further physical information on the mechanisms of polarization and dielectric relaxation in the percolation region.

II. EXPERIMENT

A. Sample preparation

We have studied an AOT-water-decane microemulsion with a composition of 17.5 vol % sodium bis(2-ethylhexyl)sulfosuccinate, 21.3 vol % water, and 61.2 vol % decane. The molar ratio of water to surfactant has the value of $W=[\text{water}]/[\text{AOT}]=26.3$. AOT and decane were purchased from Sigma and were used without further purificatoin. Deionized and bidistilled water was used throughout the experiments.

B. Experimental techniques

The general principles of TDDS and a detailed description of the setup used in our measurements have been described elsewhere [37]. The system utilizes the difference

method of measurement, with a unique registration of primary signals in a nonuniform time scale. This system permits five orders of frequency (10^5–10^{10} Hz) to overlap in one single measurement. The results can be presented both in frequency [in terms of complex dielectric permittivity $\varepsilon^*(\omega)=\varepsilon'(\omega)-\varepsilon''(\omega)$] and in time [in terms of the dielectric response function $\varphi(t)$] domains. The complex relative permittivity $\varepsilon^*(\omega)$ is related to the negative time derivative of the response function $\varphi(t)$ via the Fourier-Laplace transform

$$\varepsilon^*(\omega)=(\varepsilon_s-\varepsilon_\infty)\int_0^\infty \left[-\frac{d\varphi(t)}{dt}\right] e^{-i\omega t}dt \ , \tag{1}$$

where the real and imaginary parts of the complex dielectric permittivity are responsible for frequency-dependent polarization and energy losses, respectively. In time domain, by solving an integral equation (Eq. 4, Ref. [37]) one can obtain the results in terms of a dielectric response function $\varphi(t)=\Phi(t)+\varepsilon_\infty$ ($\Phi(t)=(\varepsilon_s-\varepsilon_\infty)[1-\psi(t)]$, where ε_s is the static dielectric permittivity, ε_∞ is the high-frequency limit, and $\psi(t)$ is the decay function of the dielectric polarization of the system). Within the framework of linear response theory it is possible to associate the decay function $\psi(t)$ with the macroscopic dipole correlation function $\Gamma(t)$,

$$\psi(t)\approx\Gamma(t)=\frac{\langle \mathbf{M}(0)\cdot\mathbf{M}(t)\rangle}{\langle \mathbf{M}(0)\cdot\mathbf{M}(0)\rangle} \ , \tag{2}$$

where $\mathbf{M}(t)$ is the macroscopic fluctuation dipole moment of the sample volume unit, which is equal to the vectorial sum of all the molecular dipoles, and the angular brackets denote averaging of the ensemble. The velocity and laws governing the correlation function $\Gamma(t)$ are directly related to the structural and kinetic properties of the sample and characterize the macroscopic properties of the system studied.

The whole procedure of measurement and data treatment in the TDDS experiment is carried out automatically. The process of control is realized in the dialog between the user and the system. The sample holders used in this experiment can be thermostabilized and the temperature can be computer controlled over the temperature range −30 °C to +100 °C.

The *TDDS measurements* were carried out in a time domain window with a total time interval of $T=750$ ns. The nonuniform sampling of the signal uses the following parameters: $T_1=15$ ns ($\delta_1=0.05$ ns), $T_2=75$ ns ($\delta_2=0.25$ ns), and $T_3=750$ ns ($\delta_3=2.5$ ns), where T_i and δ_i ($i=1,2,3$) are the time intervals used and the sampling time steps, respectively. The temperature was controlled in a thermostabilized sample holder by a cooling thermostat (Haake), accurate to ±0.2 °C. All samples were measured in a temperature range 2 °C–40 °C. The *low-frequency electrical conductivity* was measured in the temperature range 12 °C–45 °C using a conductometer manufactured by Radiometer, Copenhagen.

III. RESULTS AND DISCUSSION

A. Analysis of conductivity

The temperature dependence of the conductivity σ for AOT-water-decane microemulsions at a constant volume fraction ϕ is presented in Fig. 1. The value of the conductivity increases markedly as T is increased toward T_p.

The behavior of the electrical conductivity over a studied temperature interval can be explained as follows: Far below the percolation threshold, the conductivity of the microemulsion can be described by the charge fluctuation model [41]. In this model the conductivity is explained by the migration of charged aqueous droplets in the electric field. The droplets acquire charges owing to the fluctuating exchange of charged surfactant heads at the droplet interface and the oppositely charged counterions in the droplet interior.

In this theory, the conductivity is proportional to the volume fraction ϕ and temperature T

$$\sigma=\frac{\varepsilon_0\varepsilon k_B}{2\pi\eta r^3}T\phi \ , \tag{3}$$

where r is the droplet radius and η is the viscosity of the solvent. Our numerical calculations of the temperature dependence of the conductivity confirm the validity of this relationship up to 16 °C.

As the temperature increases above 16 °C, the charge fluctuation theory fails and the system begins to show electrical percolation behavior. On approaching the percolation threshold T_p, a power-law divergence above and below T_p can be observed:

$$\sigma\sim\begin{cases}(T_p-T)^{-s} \ , & T<T_p\\ (T-T_p)^{t} \ , & T>T_p \ .\end{cases} \tag{4}$$

The percolation threshold is observed near the temperature $T_p=25$ °C and critical indices have the values $s=1.2$ and $t=1.86$ [Fig. 2(a)].

From a theoretical point of view, static and dynamic

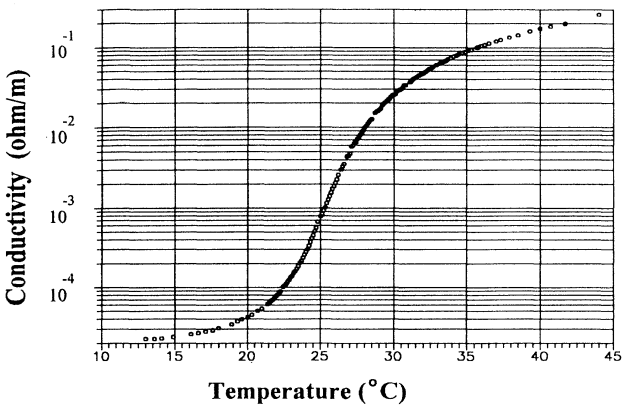

FIG. 1. Temperature dependence of the low-frequency conductivity σ for the AOT-water-decane microemulsion.

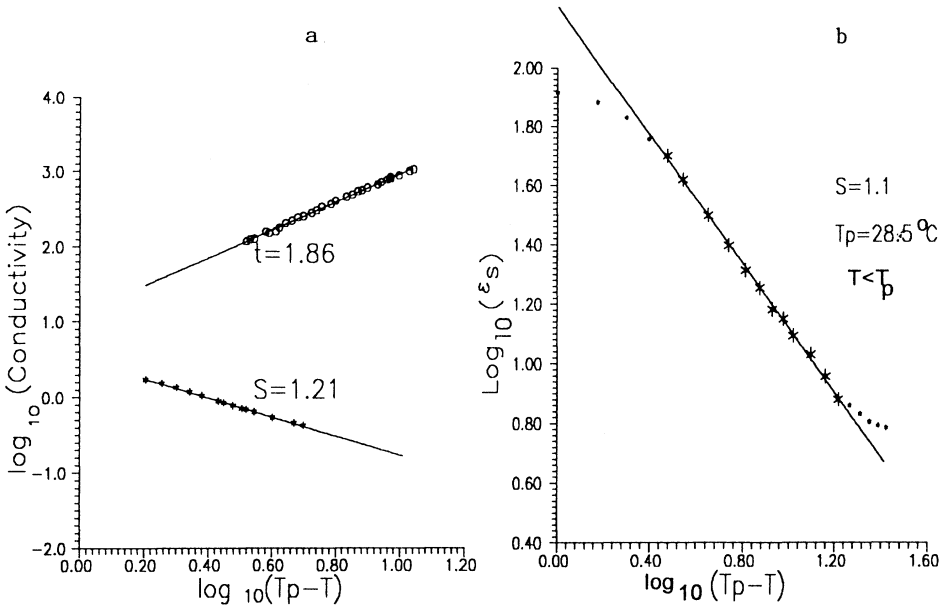

FIG. 2. Scaling behavior of (a) the conductivity and (b) the permittivity for the AOT-water-decane microemulsion below (index s) and above (index t) the percolation threshold $T_{p\sigma}=25\,^{\circ}\mathrm{C}$ (for the conductivity threshold) and $T_{p\varepsilon}=28.5\,^{\circ}\mathrm{C}$ (for the permittivity threshold).

models have been proposed for the mechanism of percolation in microemulsions. *The static percolation model* attributes this phenomenon to the appearance of bicontinuous oil and water structures [5]. Based on this model, the sharp increase of the electrical conductivity σ in such a microemulsion can be explained by the formation of a connected water path in the system.

According to the static theory of percolation, the values of the critical exponents in the regions above and below threshold should be $t\approx 1.9$ and $s\approx 0.6$, respectively. Despite the fact that these numerical values for s and t are valid for some composite materials, powders, thin films, and other materials [39,40], it was found that for microemulsions there is a disagreement of the s exponent value with the static theory value. Experimental data of critical exponents obtained by locating the percolation threshold as a function of temperature or volume fraction, for AOT-water-oil microemulsions with different types of oil (cyclohexane, dodecane, undecane, isooctane, etc.) [10–18], showed the values to be $1.1\leq s\leq 1.6$ and $1.6\leq t\leq 2.2$. Our own data concur with the above values.

The dynamic percolation model was proposed [9] in order to resolve the difficulties with the disagreement of the critical index s between the experimental data and the static percolation theory, where the theoretical value of the parameter s is equal to the experimental one ($s\approx 1.2$). This model takes into account the effect of cluster rearrangements due to Brownian motion. The value of this critical index $s=1.21$, obtained in our remeasurements for the AOT-water-decane microemulsion, indicates that dynamic percolation takes place. The value of the critical index above percolation threshold ($t=1.86$) can be interpreted according to the static as well as dynamic percolation model [8].

In a dense microemulsion system, in accordance with the dynamic percolation model, transient clusters are formed in the percolation region because of attractive interactions between droplets [42,43]. Surfactant molecules (anions) or counterions (cations) can migrate from droplet to droplet within a cluster. The correlated clusters of droplets evolve and rearrange themselves with time. It can be conjectured that two different mechanisms of transition of the charge carriers in this temperature region may take place. The first mechanism appears when droplets begin to approach or collide with each other and this mechanism is connected with the charge carriers hopping across the surfactant layers. It is presumably the main process in the scaling region below threshold T_p.

Meanwhile, in the close vicinity of the percolation threshold T_p and above, the second mechanism can also appear. It occurs when direct contacts between two or more droplets become the preferred state and droplets start to merge, so that a continuous water phase is created, forming transient water channels which charges move through.

B. Analysis of the dielectric properties

Dielectric polarization of microemulsions is a complex phenomena dependent on many factors and parameters.

Figures 3 and 4 show dielectric permittivity $\varepsilon'(\omega,T)$ and dielectric loss $\varepsilon''(\omega,T)$ dependences versus frequency and temperature. One can see that the dielectric dispersion behavior depends essentially on the temperature. In the high-frequency and low-temperature regions, the maximum of the dielectric loss has a very wide distribution. The cutoff frequency, which is defined by the beginning of the dispersion phenomenon, has much greater values in the low-temperature region than in the region near the percolation threshold.

We note that $\varepsilon'(\omega,T)$ increases sharply as T approaches the percolation threshold $T_p=28.5\,^{\circ}\mathrm{C}$, where the permittivity reaches a ridge that is essentially eminent in the low-frequency region. In the temperature region above 35 °C, on the surface of dielectric losses $\varepsilon''(\omega,T)$, it

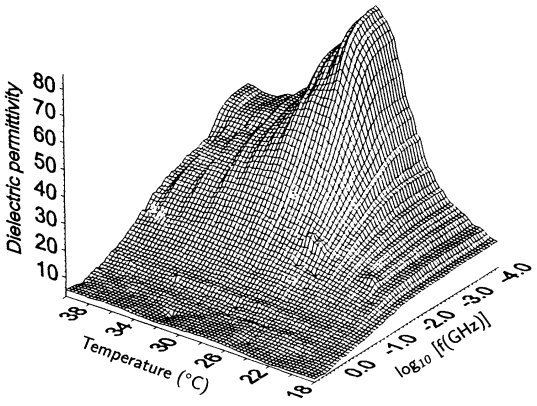

FIG. 3. Three-dimensional plots of the frequency and the temperature dependence of the dielectric permittivity ε' for the AOT-water-decane microemulsion.

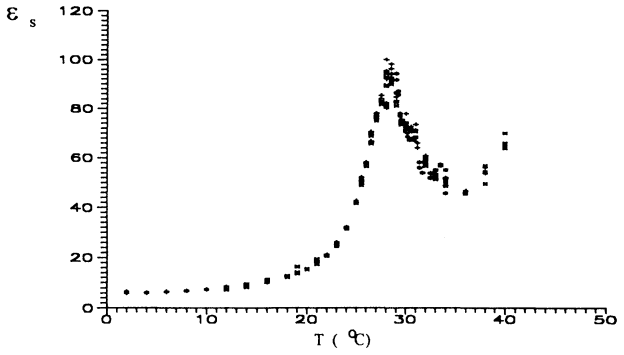

FIG. 5. The temperature dependence of the static dielectric permittivity for the AOT-water-decane microemulsion.

is possible to discern the appearance of a second peak. This peak is more prominent in the low-frequency region and on the frequency scale in this temperature region two distributed relaxation processes can be distinguished.

For detailed analyses of the frequency and the temperature behavior of dielectric permittivity and losses, let us cut a cross section of the $\varepsilon'(\omega,T)$ and $\varepsilon''(\omega,T)$ surfaces. The $\varepsilon'(\omega,T)$ cut at a constant low-frequency plane represent the temperature dependence of the low-frequency (static) dielectric permittivity versus temperature (Fig. 5). The corresponding cross sections of the $\varepsilon'(\omega,T)$ and $\varepsilon''(\omega,T)$ reliefs at constant temperature planes for the different temperatures represent the frequency dependence of the dielectric permittivity and losses for the microemulsion. Figures 6 and 7 depict the frequency dependences of dielectric permittivity and losses of the microemulsion in the percolation region ($T_p=28.5\,°C$).

In order to interpret the dielectric properties of the system being studied, let us start by analyzing *the static dielectric behavior.* The static dielectric permittivity (ε_s) behavior over the measured temperature region can be analyzed for three intervals: below the percolation threshold, in the vicinity of the percolation threshold, and above the percolation threshold.

Far below the percolation region, where our ionic microemulsion consists of separated water droplets embedded in the oil medium, the dielectric permittivity of microemulsion can be represented by the migration polarization theory of [44]. Therefore, for the dilute suspension, the static permittivity ε of a heterogeneous mixture, containing a volume fraction ϕ of suspended spherical particles of static permittivity ε_p, in a medium of permittivity ε_m ($\varepsilon_p \gg \varepsilon_m$), is given by

$$\varepsilon=\varepsilon_m+\frac{1}{3}\phi\frac{(\varepsilon_p-\varepsilon_m)(\varepsilon_m+2\varepsilon_p)}{\varepsilon_p} . \tag{5}$$

For a higher volume fraction ϕ of dispersed droplets, the relative static permittivity of the system can be better described by Hanai's theory [45]. When $\varepsilon_p \gg \varepsilon_m$, Hanai's theory provides the relationship

$$\varepsilon \cong \varepsilon_m/(1-\phi)^3 , \tag{6}$$

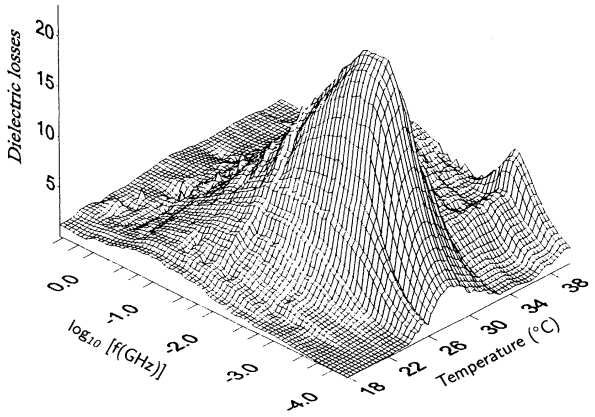

FIG. 4. Three-dimensional plots of the frequency and the temperature dependence of the dielectric losses ε'' for the AOT-water-decane microemulsion.

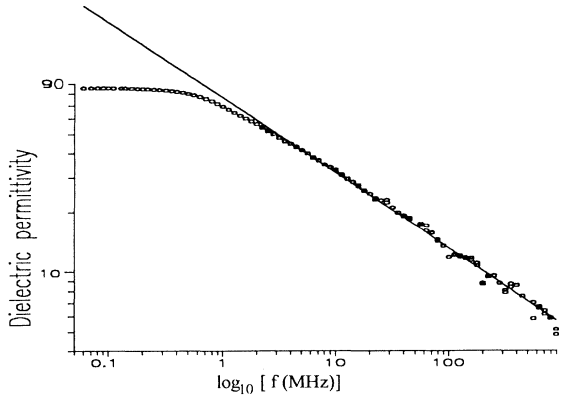

FIG. 6. Log-log plot of the frequency dependence of ε' for the AOT-water-decane microemulsion at the percolation threshold. The slopes of the linear parts correspond to $u=0.62$.

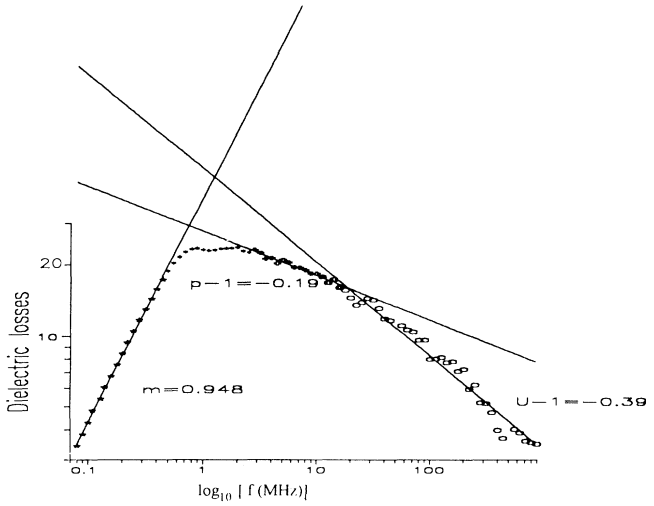

FIG. 7. Log-log plot of the frequency dependence of ε'' for the AOT-water-decane microemulsion at the percolation threshold. The slopes of the linear parts correspond to $u=0.61$, $p=0.81$, and $m=0.948$.

where in our case $\varepsilon_m=2$ (decane) and $\phi=0.388$, setting the value for dielectric permittivity ε at 8.7. This value is close to that of our experimental data in the low-temperature region.

When the temperature increases above 10 °C and reaches the percolation region, the static (low-frequency) dielectric permittivity ε_s increases in accordance with the following scaling law:

$$\varepsilon_s \sim (T_p - T)^{-s}, \quad T < T_c \ . \tag{7}$$

Figure 5 shows the temperature dependence of dielectric permittivity ε_s for an AOT-water-decane microemulsion.

From the linear regression of the dependence of $\log_{10}\varepsilon_s$ versus $\log_{10}(T_p - T)$ [Fig. 2(b)], the critical exponent can be estimated to be $s=1.1$. This result is very close to the numerical value obtained from our conductivity measurements and agrees well with the value predicted by the dynamic percolation model [9]. It is pertinent to mention here that below the percolation threshold the dielectric permittivity is much more sensitive than conductivity to structural changes in the system. This is the reason why the onset of the ε_s scaling behavior, where the coupling of the droplets begins to appear, is at ≈ 10 °C. This also explains why the onset of percolation on the temperature scale starts earlier in comparison to the onset of conductivity, which is ≈ 17 °C. On the other hand, the temperature of the conductivity percolation threshold is less than that of the permittivity threshold ($T_{p\varepsilon} > T_{p\sigma}$). This trend is similar to the case where percolation versus volume fraction was studied [10,14]. The s value obtained in our studies when we reached the percolation threshold by changing the temperature correlates well with the critical index value obtained from studies of changes in the volume fraction [10]. These results resolve the problem mentioned in earlier papers [11–14] of the discrepancies found between critical index s values for permittivity and conductivity measurements. This discrepancy was probably due to the inaccuracy involved in determining the value of the percolation threshold.

Dielectric polarization in the percolation region is presumably connected with the electrophoretic movement of charge carriers in an alternating external electric field and the charge accumulation on the interior droplet and/or cluster sides (opposite to the electrodes). In this case, the formation of an apparent fluctuating dipole moment, depending on the droplet and cluster sizes, could be responsible for the polarization of the system.

It is known that percolation clusters are self-similar [8, 38–40] and they can be modeled by fractal models. The cluster size ξ increases with the change in temperature according to the scaling power law $\xi \sim (T - T_p)^{\nu}$ [8], where ν is the critical exponent for the correlation length, which in the three-dimensional case has the numerical value $\nu=0.875$. The increase in cluster size produces an increase in the dipole moment which correlates with the permittivity growth. In the region above the percolation threshold, when the exchange of ions between droplets occurs through opened channels, the accumulation of charges would be restricted. As a result, the dipole moment of the system decreases and this can be monitored by the decrease in permittivity.

The incipient critical phenomena may affect the polarization processes. In the temperature range above 34 °C the new increase of permittivity upon increasing temperature presumably suggests that the system undergoes a structural modification. Such a change implies a transformation from an L_2 phase to L_a, corresponding to a lamellar phase [17] or to a bicontinuous one. The change of droplet shape here can occur in stages from spherical to ellipsoidal, cylindrical, and lamellar phases. The phase boundary separating the homogeneous microemulsion L_2 phase from L_a and bicontinuous phases lies at higher temperatures, beyond the temperature range of our measurements. Therefore, these transitions will not be discussed in this paper.

The dynamic aspects of the dielectric polarization may be taken into account by considering frequency dependences for dielectric permittivity and losses. The dielectric spectrum in Figs. 6 and 7 shows a rather broad dispersion in the percolation region. Various dielectric model functions have been considered appropriate to fit the dielectric spectrum [46]. These fitting functions can be represented as a sum of several Debye-type spectra $\Delta\varepsilon_j/(1+i\omega\tau_j)$, Cole-Cole $\Delta\varepsilon_j/[1+(i\omega\tau_j)\alpha]$ or Havriliak-Negami (HN) $\Delta\varepsilon_j/[1+(i\omega\tau_j)^{\alpha}]^{\gamma}$ terms, or their combinations, where $\Delta\varepsilon_j=\varepsilon_s-\varepsilon_j$ are the dielectric increments. The parameters α and γ, ranging between 0 and 1, characterize the distribution of the relaxation times.

On the other hand, it can also be observed that the curve on the Cole-Cole diagram, which represents values of $\varepsilon''(\omega)$ versus those of $\varepsilon'(\omega)$, is not an arc of a circle (Fig. 8), something which also characterizes the distribution of relaxation times. Such behavior reflects the existence of short- and long-range interactions in the vicinity of the percolation region and a hierarchy of self-

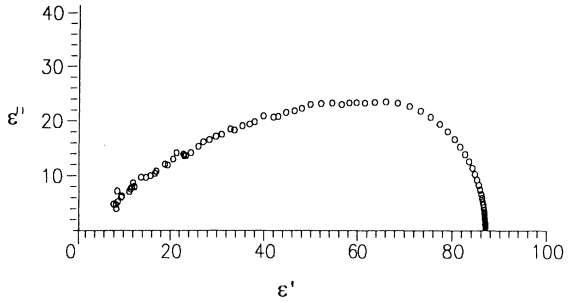

FIG. 8. Cole-Cole plot $\varepsilon''(\varepsilon')$ for the AOT-water-decane microemulsion at the percolation threshold ($T=28.5$ °C).

similar processes in the system [9,10].

The scaling concept can be applied to describe the behavior of the relaxation spectrum. The dynamic-percolation theory provides the following scaling expression for the dielectric permittivity near the threshold with respect to both the temperature and the frequency:

$$\varepsilon(T-T_p,\omega)\approx|T-T_p|^{t}f(\omega\tau_R,\omega\tau_0,|T-T_p|^{-(s+t)}) , \quad (8)$$

where $f(\omega\tau_R,\omega\tau_0,|T-T_p|^{-(s+t)})$ is the scaling function [9,22–24,47] and τ_R and τ_0 are the characteristic times describing the scaling behavior of system. τ_R is the rearrangement time of the clusters and τ_0 represents the anomalous diffusion time on the percolation cluster. In other words, τ_0 is the time needed for a charge carrier to visit all the micelles in a finite percolation cluster of size ξ, where $\tau_0\sim\xi^{(s+t)/\nu}$ [9,48]. Since the percolation clusters have a fractal nature, the rearrangements are considered to be a slow process when compared with the time needed to explore the cluster, i.e., $\tau_R\gg\tau_0$.

With respect to rearrangement motions, two regimes of behavior are expected.

(i) $\omega\tau_R\ll1$. The rearrangement occurs at times much shorter than ω^{-1}. The low-frequency dielectric permittivity gives the power-law behavior

$$(\varepsilon_s-\varepsilon')\propto\varepsilon''\propto\omega^{m} , \quad \omega<\omega_R \quad (9)$$

and the temperature scaling law (7).

(ii) $\omega\tau_R\gg1$. We expect the dielectric permittivity to be independent of τ_R. This behavior also agrees well with the dynamic scaling theory.

With respect to the characteristic time τ_0, there are also two frequency regimes where dielectric permittivity has different power-law behaviors. In the very-high-frequency region ($\omega\tau_0>1$), close to the percolation threshold, the frequency dependence of the dielectric permittivity follows the scaling behavior described by Eq. (10),

$$(\varepsilon'-\varepsilon_\infty)\propto\varepsilon''\propto(\omega\tau_0)^{u-1} , \quad \omega>\omega_0 , \quad (10)$$

where u is the scaling index. In the intermediate crossover region $1/\tau_R\ll\omega\ll1/\tau_0$, the frequency behavior of permittivity will have a more complicated character with the critical scaling index p (Fig. 7).

The scaling indices for the low- and intermediate-frequency regions, as well as for the high frequencies determined from the linear portion of the ε' and ε'' curves, can be used as a tool to compare the degrees of cooperativity of specific molecular motions in different temperature regions. Figure 9 shows a distinct temperature dependence of the low- and high-frequency parameters m and u. The empirical parameter m, determined from the linear portion of the $\log_{10}\varepsilon''$ curves, markedly deflects from 1 when the temperature approaches T_p. The region of validity of the dielectric permittivity scaling behavior for our system is narrow, which causes some difficulty in calculating accurately the temperature dependence of the parameter p in the crossover region. The evaluation of the parameter u versus temperature also shows a minimum near the percolation threshold. Consequently, the values of the parameter u for the T_p determined from the linear portion of the ε' and ε'' curves is 0.62 and 0.61, which is consistent with the other experimental studies [10,14]. The value for the parameter u obtained from the loss angle frequency dependences (Fig. 10), defined by $\tan\delta(\omega)=\varepsilon''(\omega)/\varepsilon'(\omega)$, is given by $\delta=1/2\pi(1-u)$. From Fig. 10 we obtain $\delta=0.64$; thus $u=0.59$ is in agreement with the value obtained above from the dielectric permittivity frequency dependence. It would be pertinent to note that the index value obtained in our experiments is close to the value $u=t/(s+t)=0.61$ of the R-C model of conductor-dielectric mixtures [8] and to the value $u=0.57$, derived theoretically from anomalous diffusion in the percolation clusters [48].

The temperature behavior of m, p, and u indices can be interpreted in the framework of the models based on the existence of two interwoven forms of self-similarity [49–51], one of which dominates the dielectric response at high frequencies and corresponds to the internal dynamics of clusters. The other form of self-similarity, at low frequencies, refers to the way in which the response of the macroscopic system is built up from its cluster components [49,50]. The analysis of the temperature dependences of these parameters and their fractal nature will be discussed later.

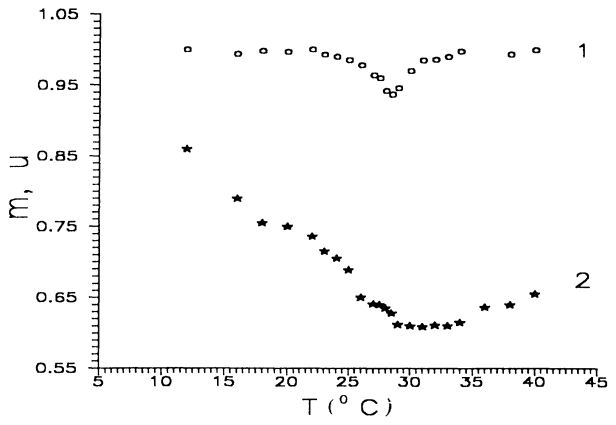

FIG. 9. Temperature dependence of the parameters m(1) and u(2) for the AOT-water-decane microemulsion.

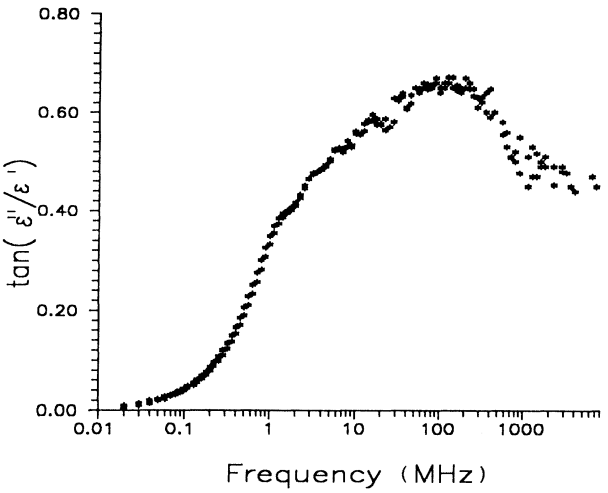

FIG. 10. Variation of the loss angle as a function of frequency for the AOT-water-decane microemulsion.

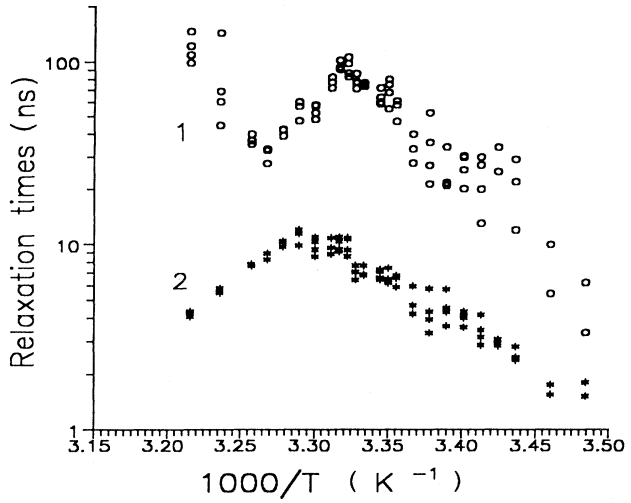

FIG. 11. Dependence of the relaxation times τ_1 and τ_2 on the reciprocal temperature [for the curves fitted using Eqs. (11) and (12)].

C. Analyses of the dipole correlation functions and the relaxation time behavior

Experience shows that the time behavior of most nonassociating dipole liquids is controlled by a single exponential decay function $\psi(t)\sim\exp[-t/\tau]$, with relaxation time τ. Associated liquids, glasses, polymers, and other multicomponent systems exhibit complex nonexponential relaxation behavior that must be deconvoluted into normal modes and represented as a sum of simple Debye exponential or Kohlrausch-Williams-Watts (KWW) nonexponential terms, such as $\psi(t)\sim\exp[-(t/\tau)^{\beta}]$. Here the parameter β characterizes the shape of the relaxation function and the cross-correlation effects, describes the morphology of the system, and can be related to different theoretical models [40, 52–55]. As mentioned elsewhere [56], there should be a connection between the parameters of the KWW and the HN functional forms; however, there is no exact analytical relationship between them.

In order to analyze the time behavior of the correlation functions, we fit them to three different decay behaviors, which can be put into the forms

$$\psi(t)=A_1\exp[-(t/\tau_1)^{\beta_1}]+A_2\exp[-t/\tau_2]\ , \tag{11}$$

$$\psi(t)=A_1\exp[-t/\tau_1]+A_2\exp[-(t/\tau_2)^{\beta_2}]\ , \tag{12}$$

$$\psi(t)=A_1\exp[-(t/\tau_1)^{\beta_1}]+A_2\exp[-(t/\tau)^{\beta_2}]\ , \tag{13}$$

where τ_i are the relaxation times and A_i are the amplitudes of the processes ($i=1,2$). Equation (13) reduces to (11) or (12), when β_2 or β_1 equals 1.

A best fitting of each curve to Eqs. (11)–(13) was performed by a least-squares procedure where one found the corresponding parameters A_i,τ_i,β_i ($i=1,2$) and the minimum standard deviation χ^2. The quality of each fit to Eqs. (11)–(13) was established by comparing the obtained χ^2 minimum.

Figure 11 plots the temperature dependences of the relaxation times versus the revised temperature for the curve fitted by Eq. (11). The analysis of the dependence of the relaxation times τ_1 and τ_2 on temperature shows a similar time behavior for all three fitting decay functions (11)–(13).

As has been mentioned above, on the frequency scale (Figs. 3 and 4) a broadly distributed relaxation process can be discerned in the low-temperature (below the percolation region) and high-frequency regions. The corresponding fitting relaxation times τ_1 and τ_2 have the values of a few nanoseconds and are close to each other on the time scale. We assume that it is just one very broadly distributed relaxation process.

In the percolation threshold region the relaxation times exhibit a maximum obtained for the same value of T corresponding to the maximum of the static permittivity. The effective activation energy above percolation threshold, obtained from the curve of the dependence of relaxation times τ_1 and τ_2 on reciprocal temperature, have the values 160 and 120 kJ/mol, respectively. These rather large energy values correlate with the activation energy of the clustering of two droplets [14] and with the activation energy of the H_2O–self-diffusion coefficient of the water-AOT-hydrocarbon microemulsions [18] in the percolation region as well.

The second peak, which is clearly eminent on the frequency scale at temperatures above 34 °C (Fig. 4), corresponds to the appearance of a new relaxation process. This relaxation process shows reverse Arrhenius behavior and depends on the structural changes occurring in the system. The appearance of this process at high temperatures, as well as the increase in static permittivity mentioned above, testifies to the onset of the transition to the lamellar or the bicontinuous phase.

Given the complexity of the chemical makeup of microemulsions, a precise interpretation of the dielectric relaxation mode is difficult. To understand the dielectric

spectrum of microemulsions, it is necessary to analyze dielectric information from the various sources of the relaxations. The dynamic processes, depending on their nature, can be classified by two types: The first type characterizes the droplet and percolation cluster behavior and is connected with their translations, rotations, collisions, fusion, fission, and shape fluctuations [57] as well. The second type of relaxation processes reflects some characteristics inherent to the dynamics of the single-particle components. Since our system is ionic, the dielectric relaxation contributions of this type are expected to be related to the processes connected to the interfacial polarization, counterion polarization resulting from the movement of ions and/or surfactant counterions relative to the droplets, and their organized clusters and interfaces. The relaxation can also be related to various components of the system containing active dipole groups, such as bound and free water. All these contributions can cause complex dielectric behavior.

In order to ascertain the origins and mechanisms responsible for the obtained relaxation times, let us compare the magnitudes of τ_1 and τ_2 with the characteristic times related to various physical processes that occur in heterogeneous systems.

The droplet collision time, associated with a rearrangement process, can be estimated [58] according to the relationship

$$\tau_{\text{coll}} \sim 3\pi\eta R^3/4\phi k_B T \ , \tag{14}$$

where R is the radius of the dispersed particles (in our case it is a water core plus shell), η is the viscosity of the medium, ϕ is the volume fraction of the dispersed phase, and $k_B T$ is the thermal energy term. The average radius R_w of the water core is related to W by a semiempirical relation $R_w = (1.25W + 2.7)$ Å [17]. The radius R of the surfactant-coated water droplet (the AOT chain length is 12 Å) is estimated to be 50 Å. For $\eta = 0.8$ cP (decane at 20 °C), the collisional times are estimated to be about 200 ns.

The relaxation time associated with *the translational and the rotational diffusion* of a spherical permanent dipole, according to Debye [59,60], is given by

$$\tau_{\text{tr}} \sim R^2/D \sim 6\pi\eta R^3/k_B T \ , \tag{15}$$

$$\tau_{\text{rot}} = 4\pi\eta R^3/k_B T \ , \tag{16}$$

where D is the diffusion coefficient. In our case the dipole orientation relaxation times are about 300–350 ns, which exceed, by roughly one and two orders of magnitude, the τ_1 and τ_2 derived from experimental data.

A thermal shape fluctuation of the microemulsion droplets, which distorts them from their average spherical form, can contribute to the relaxation dispersion of the system [57,61,62]. The lowest dominant mode of bending elasticity has a relaxation time given by

$$\tau_{\text{SF}} \sim \eta R^3/K_c \sim \eta R^3/5k_B T \ , \tag{17}$$

where K_c is the elastic curvature module of a spherical droplet, which was estimated [62] to be $5k_B T$. The thermal shape fluctuation mode has a magnitude of 5 ns and is able to contribute to the relaxation spectrum in the region below percolation, when droplets are not fused and their average radius is not changed. In the vicinity of the percolation threshold, when the droplets form clusters, they change their shape and increase their radius. It can also lead to the increase of the time magnitude.

For a mixture of two or more components, it is evident that each phase undergoes its own dielectric relaxation. However, in addition to this, the accumulation of charges at the oil/water interface gives rise to polarization and contributes to relaxation when at least one component is electrically conductive. This phenomenon is know as *interfacial polarization* or the *Maxwell-Wagner-Sillars (MWS) effect* [63,59]. The MWS equation for the relaxation time of the interfacial polarization for spherical particles is given by

$$\tau_{\text{MWS}} = \frac{2\varepsilon_m + \varepsilon_p + \phi(\varepsilon_m - \varepsilon_p)}{2\sigma_m + \sigma_p + \phi(\sigma_m - \sigma_p)}\varepsilon_0 \ , \tag{18}$$

where ε_0 is the dielectric constant, $\varepsilon_p, \varepsilon_m$ are dielectric permittivities, and σ_p, σ_m are the specific electrical conductance of the dispersed phase and the medium, respectively.

To calculate the relaxation time responsible for the MWS effect we assume a set of parameters as follows: $\varepsilon_0 = 8.85 \times 10^{-12}$ F m^{-1}, $\varepsilon_p = 78$, $\varepsilon_m = 2$, $\sigma_p = 1.23$ mho/m, $\sigma_m < 10^{-6}$ mho/m, and $\phi = 0.388$. Here the specific conductivity of the dispersed phase σ_p was estimated from the slope of the scaling expression (19) for conductivity of the system σ versus volume fraction of the dispersed phase ϕ far above the percolation threshold [20]:

$$\sigma = \tfrac{3}{2}\sigma_p(\phi - \tfrac{1}{3}) \ . \tag{19}$$

We calculated the relaxation time of the MWS effect to be 0.62 ns, which is smaller than the observed relaxation times in the percolation region. However, it is very close to the average relaxation time (~ 0.5–0.8 ns) in the low-temperature region 2 °C–13 °C.

Since our microemulsion is a three-component system consisting of a water core surrounded by a monomolecular surfactant shell dispersed in an oil phase, the dielectric relaxation of this dispersion with shells can be described by *the triphasic model of interfacial polarization* [63–65] instead of the MWS model. This model predicts the occurrences of two different dielectric dispersions under the conditions $\sigma_m \ll \sigma_s$ and $\sigma_m \ll \sigma_p$. Assume the approximate expressions for relaxation times

$$\tau_1 = \frac{\varepsilon_s}{\sigma_s}\varepsilon_0 \tag{20}$$

and

$$\tau_2 = \frac{\varepsilon_p + (2d/R_w)\varepsilon_s}{\sigma_p + (4d/R_w)\sigma_s}\varepsilon_0 \ , \tag{21}$$

where $R_w = 36$ Å is the radius of a water core surrounded by a shell of thickness $d = 12$ Å, specific conductivity $\sigma_s \approx 10^{-3}$ mho/m, and dielectric permittivity $\varepsilon_s = 3.2$ [64]. Equations (20) and (21) yield relaxation times of

about $\tau_1 \sim 28$ ns and $\tau_2 \sim 0.58$ ns.

For the present system, the relaxation time given by O'Konski's model, which includes the effect of surface conductivity [65], is nearly identical to the time given by the MWS theory and the smaller time of the triphasic model of interfacial polarization.

The theory of double-layer polarization [66], together with *the triphasic model of interfacial polarization* where the shell phase is taken as the electric double layer [59], consider both the dispersion due to counterion displacement in the double layer and the interfacial polarization. They are given by the following expressions for the relaxation times:

$$\tau_1 = \frac{e_0^2 \rho_0 R_w^2}{2 k_B T \lambda_0} \tag{22}$$

and

$$\tau_2 \approx \frac{\varepsilon_p}{\sigma_p} \varepsilon_0 + \frac{e_0^2 R_w \rho_0}{k_B T \sigma_p} , \tag{23}$$

where e_0 is the charge of one electron, ρ_0 is the surface charge density, and λ_0 is the surface conductivity [65]. For an average water droplet of 36 Å radius, there are approximately 110 anionic surfactant molecules on the interface. The surface charge density corresponding to the full ionization of the AOT molecules is estimated to be 6×10^{17} elementary charges per 1 m^2 and the surface conductivity $\approx 0.9 \times 10^{-9}$ mho [64,59]. It is relevant to emphasize here that the validity of using Eqs. (18) and (19) is limited to the region below percolation, where droplets are separated from each other, do not merge, and their radii remain unchanged. The relaxation times calculated on the basis of Eqs. (22) and (23) at $T = 10\,^{\circ}\mathrm{C}$ are $\tau_1 \sim 29$ ns and $\tau_2 \sim 12$ ns.

We can see that the dielectric relaxation time τ_1 calculated on the basis of this combined theory as well as on the triphasic model of interfacial polarization is larger by a factor of 30 than experimental results. The high-frequency relaxation time τ_2, corresponding to the relaxation between a droplet with its double layer and the medium, is an order of magnitude higher than the corresponding time calculated from the MWS and the triphasic model of interfacial polarization, as well as the experimental value.

In order to complete the discussion of models responsible for the high-frequency dispersion, it is also worth mentioning in this list the model of dielectric *polarization of bound water,* which can contribute to the observed relaxation picture, as well as the mechanism proposed by Cametti, Codastefano, and Tartaglia [64]. Cametti, Codastefano, and Tartaglia associated the high-frequency dispersion characterized by a relaxation time of the order of 10^{-10} s, and in their case largely independent of temperature, with the *collective motions of the anionic head groups of the surfactant molecules* at the interface with the water phase.

A perusal of the relaxation time values shows that, in the temperature region below percolation, within the accuracy of the estimations, a widely distributed relaxation process takes place. The values of corresponding relaxation time in this temperature region obtained in our fitting have weak dependence on T. The values of the relaxation time, as well as the values of static dielectric permittivity mentioned above, are in agreement with the data that the interfacial polarization models provide. All these models, which describe the polarization process of the system, show the values of the relaxation times to be close to each other. Meanwhile, in the close vicinity of the percolation threshold, the widely distributed relaxation time splits up at the two separated distributed times.

A long relaxation process involves rearrangements and movements of the droplets forming the clusters. The experimental value τ_1 has a broad distribution and it is close to the magnitude of the estimated collision time τ_{coll}. A steep increase in the value of the amplitude A_1 of the long relaxation time τ_1 (see Fig. 12) testifies that this process becomes more active in the percolation region. The magnitude of τ_1 drastically increases when temperature approaches T_p (Fig. 11), which also hints at a dependence of the long relaxation time on the size of the clusters.

In the percolation region a short experimental time τ_2 coincides well with the shape fluctuation mode. The shape fluctuation processes in themselves are not dielectrically active; however, they can affect diffusion of the charge carriers both in the water bulk and at the interface and contribute mainly to the fast relaxation processes. When temperature nears the percolation threshold and droplets approach each other, the effective cluster size increases and therefore retards the vibration mode.

Temperature variations cause numerous effects and processes that occur in the system, i.e., changes in the local medium viscosity, in the AOT aggregation number, in the shape and radius of droplets, in the elastic curvature module of a spherical droplet, etc. In the framework of existing models, one must be very careful when speculating quantitatively about the evaluation of relaxation times versus temperature and attempting to explain the

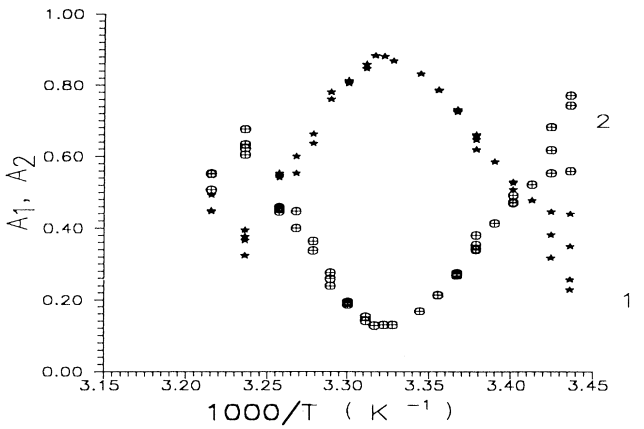

FIG. 12. Dependence of the amplitudes of the relaxation processes 1 and 2 on the reciprocal temperature [for the curves fitted using Eq. (13)].

time versus temperature dependences, especially in the vicinity of the percolation threshold.

D. Fractal concepts for dielectric relaxation

The frequency scaling parameters (m, p, and u), as well as stretched parameters in the time window (β_1 and β_2), provide information about the microstructure and dynamics of the system. An interpretation of these parameters in terms of diffusion or Brownian motion problems on fractal clusters [48] can suggest a general mechanism of the relaxation phenomena in the percolation region regardless of the microscopic details of the sample. Thus the fractional power law of a dielectric permittivity versus frequency and correlation functions versus time could be understood as the macroscopic manifestation of self-similarity on the microscopic level of the system.

Recently, a number of the models have been advanced [49–52, 67–73] that describe the deviation of the dynamic behavior of the systems from the Debye exponential relaxation law. Despite differences in physical details and nature, the proposed models are based on a hierarchy of self-similar processes and reflect a scale-invariant distribution of relaxation times. The scale invariance in space is connected with the temporal and energetic ones, as spatial, temporal, and energetic correlations cannot exist independently.

In order to understand the scaling nature of the relaxation behavior of percolation clusters, the diffusion in a fractal medium must be considered. The arrangement of various clusters in the percolation region may be defined by the fractal dimensionality D_f. The magnitude of D_f depends on the degree of disorder present in the system and shows the scaling mass M dependence on distance L [$M(L) \sim L^{D_f}$].

A dielectric polarization phenomenon in the disordered structure can be related to the diffusion of a random walker which, in the case of diffusion in the percolation cluster, does not go on in the same way as in Euclidean space. The mean-square displacement time behavior $\langle R^2(t) \rangle \sim t^a$ in this case also does not obey the Brownian motion ($a=1$) law [48,67]. A random walk on model spatial deterministic fractals (e.g., Sierpinski gaskets) [67], where the temporal aspect is ordered, yields an anomalous diffusion with $a = D_s / D_f < 1$, where D_s is the spectral dimension of the cluster [8,67].

On the other hand, for a random walker that pauses for a random time between jumps, if the waiting time density behaves asymptotically as the inverse power law $t^{-1-\gamma}$, with $0 < \gamma < 1$ (γ is the degree of temporal homogeneity, which is also called a fractal dimension D_t of the time process [40,74]), Blumen *et al.* [52] obtained the expression for the mean-square displacement time dependence $\langle R^2(t) \rangle \sim t^{a\gamma}$. In this dependence, two parameters characterizing the spatial and time disorders in the system are combined multiplicatively. Such pauses between the jumps can be, for instance, due to motion in a disordered system with a random distribution of the activation barriers.

For a system with spatial and temporal disorder, Blumen *et al.* [52] also obtained the relationship between a stretched parameter β of the decay behavior $\psi(t) \sim \exp[-(t/\tau)^{\beta}]$ and an exponent of the power law for the $\langle R^2(t) \rangle$ time dependence as follows:

$$\beta = \begin{cases} \gamma D_f a/2 , & aD_f < 2 \\ \gamma , & aD_f > 2 . \end{cases} \tag{24}$$

For anomalous diffusion in a three-dimensional percolation lattice at the percolation threshold, this expression has [33] a very simple form, $\beta \approx 0.65\gamma$, which can be useful for an analysis of values of the experimental stretched exponents.

Diffusion motion, which is faster than normal Brownian motion, can be described in terms of the existence of energetic disorder and turbulent motions [33,53–55]. The approach is based on the fractal properties of the free-energy surface, i.e., on the existence of the ultrametric space for the energy of barriers. In this case, depending on the parameters of the ultrametric space of the energy barriers, diffusion can be inhibited or enhanced (the corresponding exponent of the mean-square displacement time dependence and the stretched exponent of the correlation functions are lesser or greater than unity). On the other hand, theoretical models that operate in the frequency window also yield relationships between frequency scaling parameters and fractal exponents and combine them multiplicatively. In this case, at least to a good approximation for the high-frequency scaling parameter, it has been suggested [40,52] that $1-u = D_t D_s/2$. In their turn, the indices p and m are expected [40,75] to be connected with D_t.

The appearance of temporal disorder in the system in the close vicinity of the percolation region is manifested by the deflection of the parameter m from unity ($m \sim 0.94$) (Fig. 9). In its turn, the parameter u reflects the existence of spatial, temporal, and possibly also energetic disorder in the system. However, it is easier to deliberate about such dependences in terms of the parameters β_1 and β_2.

The variation behaviors of the frequency scaling parameters m and u (Fig. 9) and stretched exponents β_1 and β_2 as functions of the temperature (Fig. 13) indicate morphological changes in the system and serve to differentiate the mechanism underlying the relaxation among numerous physical processes occurring in the system. As mentioned above, at the low-temperature region ($< 16\,^{\circ}\mathrm{C}$) a polarization of the system provides one widely distributed process. The corresponding stretched parameter β_1 in this case is equal to 0.4, with an error margin of 0.1. This rather low value of the stretched parameter β_1 in the temperature region implies the existence of a few relaxation mechanisms occurring in the system. These mechanisms can be associated with interface polarization and mobility of ions in the interface and water bulk of the microdroplets.

Figure 13 presents the stretched exponent dependences on the temperature in the percolation region extracted from relationships (11)–(13). It is clear from this figure that when the temperature reaches the percolation threshold, the stretched exponent of the slow relaxation process β_1 has a maximum magnitude of 0.72 ± 0.03. On

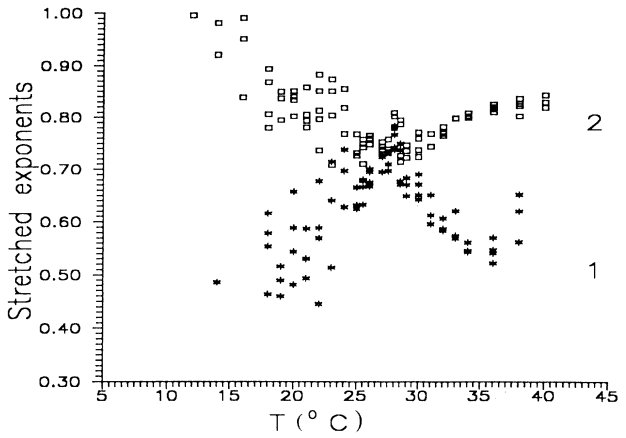

FIG. 13. Temperature dependence of the stretched exponents β_1 [fitted using Eq. (11)] and β_2 [fitted using Eq. (12)].

the other hand, the value of the stretched exponent of the fast relaxation process β_2 generally decreases as T increases from unity (at the onset of the percolation region) and shows a minimum of 0.73 ± 0.03 (at the percolation threshold T_p), i.e., has the same mean value that is reached by β_1.

In terms of the fractal picture, the results of the low value of β_1 at the temperatures corresponding to the beginning of the percolation region can be connected with a broad size distribution of droplets and seem to indicate that a rearrangement process with strong cooperative movement of the droplets is taking place in the system. In the vicinity of T_p, an increase of the stretched parameter β_1 can be explained by the appearance of the enhanced diffusion that predominates over the contribution of the temporal disorder. For a microemulsion analogous to ours the fractal time dimension characterizing the temporal disorder in the system at the percolation threshold was estimated to be ~0.7 [33]. For this reason, our relatively large value of the stretched parameter ($\beta_1\sim0.72$) at T_p, in accordance with relationship (24), can be interpreted as the existence not only of a temporal disorder, but also of an energetic disorder for the energy barriers associated with the fusion-fission processes for the droplet-droplet and droplet-charge bonds within clusters. The decrease of β_1 above the percolation threshold can be related to the changes of morphology of the microemulsion and the increase of cooperative movements within it. Such a change of character of the mobility and dimensionality in the system can be related to the involvement of the rearrangement processes of the large clusters that appear in the percolation region.

The decrease of the stretched parameter of the fast relaxation process β_2 can be connected with variation of the diffusion mechanism that is deviating from normal behavior at low temperatures ($\beta_2\sim1$) to the anomalous one at T_p. The coincidence of the values β_1 and β_2 to each other in the percolation threshold means that in this temperature region the same law of anomalous diffusion of charge carriers governs the processes of polarization in the microemulsion on the two time scales. Above the percolation threshold the system approaches ordinary diffusion behavior; however, it does not attain it, which is manifested by the slight increase of β_2.

IV. CONCLUSIONS

The above dielectric relaxation study of the AOT-water-decane microemulsion near the percolation temperature threshold leads to the following general conclusions.

(i) The critical indices for σ and ε have the values $s\approx1.2$ below and $t\approx1.9$ above the percolation threshold. The value of critical index s is in agreement with the dynamic percolation model. This confirms the idea that the mechanism responsible for the temperature dependence of conductivity and permittivity has the same origin.

(ii) In the temperature region below percolation the values of the distributed relaxation time, which describes the polarization process of the system, as well as the values of static dielectric permittivity are in agreement with the data that the interfacial polarization models provide.

(iii) In the close vicinity of the percolation threshold, the distributed relaxation time splits up into two separate times. In the percolation region, the long relaxation process involves rearrangements and movements of the droplets forming the clusters. The short experimental time is responsible for the shape fluctuation mode.

(iv) The fractional power law of dielectric permittivity versus frequency and correlation functions versus time can be understood as the macroscopic manifestation of self-similarity at the microscopic level of the system.

(v) The frequency scaling parameters m, p, and u, as well as the stretched β parameters in the time window, provide information about the microstructure and dynamics of the system. In addition, they show the existence of spatial, temporal, and energetic disorders associated with anomalous diffusion of charge carriers in the percolation clusters. The interpretation of these parameters in terms of fractal concepts offers a general mechanism of the relaxation phenomena in the percolation region regardless of the microscope details of the sample.

ACKNOWLEDGMENTS

The authors would like to express their appreciation to Professor Sam Safran (Weizmann Institute), Professor Haim Halpern (Bar-Ilan University), and Professor Avinoam Ben-Shaul (Hebrew University) for reading the manuscript and for helpful discussions. One of us (Yu.F.) acknowledges the support of the Wulfson Foundation and of Grant No. 3499 from the Israel Minister of Science and Technology.

[1] S. E. Friberg, *Microemulsions: Structure and Dynamics* (CRC, Boca Raton, FL, 1987), p. 219.
[2] *Surfactants, Adsorption, Surface Spectroscopy and Disperse Systems,* edited by B. Lindman (Steinkopff, Darmstadt, 1985), p. 127.
[3] D. Langevin, Annu. Rev. Phys. Chem. **43**, 341 (1992).
[4] U. Olsson, K. Shinoda, and B. Lindman, J. Phys. Chem. **90**, 4083 (1986).
[5] P. G. De Gennes and C. Touplin, J. Phys. Chem. **86**, 2294 (1982).
[6] M. Kotlarchyk, S. H. Chen, J. S. Huang, and M. W. Kim, Phys. Rev. A **28**, 508 (1983).
[7] S. Chen, T. Lin, and J. S. Huang, in *Physics of Complex and Supramolecular Fluids,* edited by S. Safran and N. Clark (Wiley, New York, 1987).
[8] J. P. Clerc, G. Giraud, J. Laugier, and J. Luck, Adv. Phys. **39**, 191 (1990).
[9] G. Grest, I. Webman, S. Safran, and A. Bug, Phys. Rev. A **33**, 2842 (1986).
[10] A. Ponton and T. K. Bose, J. Chem. Phys. **94**, 6879 (1991).
[11] S. Bhattacharya, J. P. Stokes, M. W. Kim, and J. S. Huang, Phys. Rev. Lett. **55**, 1884 (1985).
[12] M. W. Kim and J. S. Huang, Phys. Rev. A **34**, 719 (1986).
[13] M. A. Dijk, Phys. Rev. Lett. **55**, 1003 (1985).
[14] M. A. Dijk, G. Casteleijn, J. G. H. Joosten, and Y. K. Levine, J. Chem. Phys. **85**, 626 (1986).
[15] C. Cametti, P. Codastefano, A. Di Biasio, P. Tartaglia, and S. Chen, Phys. Rev. A **40**, 1962 (1989).
[16] C. Cametti, P. Codastefano, P. Tartaglia, J. Rouch, and S. Chen, Phys. Rev. Lett. **64**, 1461 (1990).
[17] C. Cametti, P. Codastefano, P. Tartaglia, S. Chen, and J. Rouch, Phys. Rev. A **45**, R5358 (1992).
[18] H. F. Eicke, R. Hilfiker, and M. Holz, Helv. Chim. Acta **67** (2), 361 (1984).
[19] A. Maitra, Ch. Mathew, and M. J. Varshney, J. Phys. Chemn. **94**, 5291 (1990).
[20] S. Bisal, P. K. Bhattacharya, and S. P. Moulik, J. Phys. Chem. **94**, 350 (1990).
[21] J. Peyrelasse, M. Moha-Ouchane, and C. Boned, Phys. Rev. A **38**, 904 (1988).
[22] C. Mathew, Z. Saidi, J. Peyrelasse, and C. Boned, Phys. Rev. A **43**, 873 (1991).
[23] J. Peyrelasse and C. Boned, Phys. Rev. A **41**, 938 (1990).
[24] C. Boned, J. Peyrelasse, and Z. Saidi, Phys. Rev. E **47**, 468 (1993).
[25] M. Clarkson, Phys. Rev. A **37**, 2070 (1988); **37**, 2079 (1988).
[26] A. Jada, J. Lang, R. Zana, R. Makhloufi, E. Hirsch, and S. Candau, J. Phys. Chem. **94**, 387 (1990).
[27] J. Lang, N. Lalem, and R. Zana, J. Chem. Phys. **95**, 9533 (1991); **96**, 4667 (1992).
[28] J. Lang and R. Zana, in *Surfactant Solutions: New Methods of Investigations,* edited by R. Zana, Surfactant Reactant Sciences Series Vol. 22 (Dekker, New York, 1987), p. 405.
[29] R. Zana, in *Surfactant Solutions: New Methods of Investigation* (Ref. [28]), p. 241.
[30] J. Xu and G. Stell, J. Chem. Phys. **889**, 1101 (1988).
[31] M. S. Skaf and G. Stell, Phys. Rev. A **46**, R3020 (1992).
[32] M. S. Skaff and G. Stell, J. Phys. A **26**, 1051 (1993).
[33] M. A. Lopez-Quintela and D. Losada, Phys. Rev. Lett. **61**, 1131 (1988).
[34] M. A. Lopez-Quintela, J. Rivas, D. Losada, and J. I. Lopez Cabido, J. Non-Cryst. Solids **131-133**, 229 (1991).
[35] J. Lang, A. Jada, and A. Malliaris, J. Phys. Chem. **92**, 1946 (1988).
[36] B. Lindmann, T. Ahlnas, O. Soderman, and H. Wiolderhang, Faraday Discuss. Chem. Soc. **76**, 317 (1983).
[37] Yu. Feldman, Yu. Zuev, E. Polygalov, and V. Fedotov, Colloid Polym. Sci. **270**, 768 (1992).
[38] H. Takayasu, *Fractals in the Physical Sciences* (Wiley, New York, 1990), p. 170.
[39] A. L. Efros and B. I. Schklovskii, Phys. Status Solidi B **76**, 475 (1976).
[40] G. Niklasson, K. Brantervik, and I. Serbinov, in *Time-Dependent Effect in Disordered Materials,* edited by Roger Pynn and Tormod Riste (Plenum, New York, 1987), p. 107; G. A. Niklasson, J. Appl. Phys. **62**, R1 (1987).
[41] H. F. Eicke, M. Bercovec, and B. Das-Gupta, J. Phys. Chem. **93**, 314 (1989).
[42] S. A. Safran, I. Webman, and G. S. Grest, Phys. Rev. A **32**, 506 (1985).
[43] A. L. R. Bug, S. A. Safran, G. S. Grest, and I. Webman, Phys. Rev. Lett. **55**, 1896 (1985).
[44] J. Sjoblom and B. Gestblom, in *Organized Solutions. Surfactants in Science and Technology,* edited by S. E. Friberg, and B. Lindman (Dekker, New York, 1992), p. 193.
[45] T. Hanai, Kolloid-Z. **171**, 23 (1960).
[46] S. Havriliak, Jr. and S. J. Havriliak, J. Mol. Liq. **56**, 49 (1993).
[47] D. Stroud and D. J. Bergman, Phys. Rev. B **25**, 2061 (1982).
[48] Y. Gefen, A. Aharony, and S. Alexander, Phys. Rev. Lett. **50**, 77 (1983).
[49] L. A. Dissado and R. M. Hill, Chem. Phys. **111**, 193 (1987).
[50] L. A. Dissado and R. M. Hill, J. Appl. Phys. **66**, 2511 (1989).
[51] L. A. Dissado and J. M. Alison, J. Mol. Liq. **56**, 295 (1993).
[52] A. Blumen, J. Klafter, B. S. White, and G. Zumofen, Phys. Rev. Lett. **53**, 1301 (1984).
[53] W. P. Keirstead and B. A. Huberman, Phys. Rev. A **36**, 5392 (1987).
[54] S. Havlin, B. L. Trus, and G. H. Weiss, J. Phys. A **19**, L817 (1986).
[55] F. Wegner and S. Grossmann, Z. Phys. B **59**, 197 (1985).
[56] F. Alvarez, A. Alegria, and J. Comenero, Phys. Rev. B **44**, 7306 (1991).
[57] S. A. Safran, J. Chem. Phys. **78**, 2073 (1983).
[58] G. D'Arrigo, A. Paparelli, A. D'Aprano, I. D. Donato, M. Goffredi, and V. T. Liveri, J. Phys. Chem. **93**, 8367 (1989).
[59] S. I. Chou and D. O. Shah, J. Phys. Chem. **85**, 1480 (1981).
[60] P. J. Debye, *Polar Molecules* (The Chemical Catalog Co., New York, 1929).
[61] S. T. Milner and S. A. Safran, Phys. Rev. A **36**, 4371 (1987).
[62] J. S. Huang and S. T. Milner, Phys. Rev. Lett. **59**, 2600 (1987).
[63] T. Hanai, in *Emulsion Science,* edited by P. Sherman (Academic, New York, 1968), p. 353.
[64] C. Cametti, P. Codastefano, and P. Tartaglia, Ber. Bunsenges. Phys. Chem. **94**, 1499 (1990).
[65] Ch. O'Konski, J. Chem. Phys. **64**, 605 (1960).
[66] S. S. Dukhin and V. N. Shilov, *Dielectric Phenomenon and the Double Layer in Disperse Systems and Polyelectrolytes,* translated by D. Lederman (Halsted, New York, 1974).
[67] S. Havlin and D. Ben-Avraham, Adv. Phys. **36**, 695 (1987).

[68] K. Weron and A. Jurlewicz, J. Phys. A **26**, 395 (1993).
[69] K. L. Ngai and R. W. Rendell, J. Mol. Liq. **56**, 199 (1993).
[70] J. Klafter and M. F. Shlesinger, Proc. Natl. Acad. Sci. U.S.A. **83**, 848 (1986).
[71] E. Y. Sheu, S.-H. Chen, J. S. Huang, and J. C. Sung, Phys. Rev. A **39**, 5867 (1989).
[72] S.-H. Chen, J. Rouch, and P. Tartaglia, J. Non-Cryst. Solids **131-133**, 275 (1991).
[73] R. G. Palmer, D. L. Stein, E. Abrahams, and P. W. Anderson, Phys. Rev. Lett. **53**, 958 (1984).
[74] M. Massalska-Arodz, Mol. Cryst. Liq. Cryst. **214**, 171 (1992).
[75] K. Brantervik and G. Niklasson, Thin Solid Films **165**, 67 (1988).